ISSN:2566-3143, eISSN:2566-3151, DOI: 10.2478/bhee-2026-0020

DTS: AN INNOVATIVE SYNCHRONIZATION METHOD FOR SYNCHRONOUS CONDENSER WITH THE ELECTRICAL GRID

Domenico Tedeschi[1], Roberto Benato[2], Francesco Sanniti[2], Luca Rusalen[2]

Abstract: This paper presents an original deterministic approach to improve the success rate of the synchronization process of a synchronous condenser. In fact, the start-up process of a synchronous condenser cannot rely on the presence of a supply system to regulate its speed during the synchronization process, as happens with traditional synchronous generators. A static frequency converter is used to start the machine, but it should be disconnected before the grid synchronization to avoid damage, making the process uncontrollable. The proposed method aims to analytically determine the optimal frequency and phase angle to disconnect the converter to ensure synchronization with the grid within proper thresholds. The accuracy of the method is confirmed by a comparison with on-field recording of real synchronous condenser start-up processes. This procedure enables significantly reducing the frequency threshold for the synchronization so to limit the thermal and mechanical stresses of the machine and to increase its lifecycle.

Keywords: Synchronous condenser, synchronization process, machine start-up.

INTRODUCTION

The Synchronous Condenser (SC) technology has been exploited for decades in power systems to improve voltage regulation and stability by continuously rebounding reactive power with the network. In the last years, the increasing penetration of inverter-based Renewable Energy Sources (RESs) in the energy mix fostered interest in SC technology [1]. For these reasons, the Transmission System Operators (TSOs) all over the world are rediscovering the benefits of conventional SC technology and are looking for ways to install them in their networks from a technical and economical perspective. [2]–[4].

In Europe, more than 10 large SC plants have been connected since 2012 to support Danish, German, and Italian power systems, 20 new SC plants have been installed in North America, 5 in Australia and more than 10 in Asia [5]. In the next ten years, more than 20 new installations are commissioned in Europe by the main national TSOs [6]–[9] .

The installation of SC is a benefit for the power systems stability in terms of:

- System inertia: Inertia is an inherent feature of a SC since it is a rotating machine. The benefit of inertia is improved voltage ‘stiffness’, which improves the overall behaviour of the system. Typically, SCs are coupled with a flywheel system, to increase the inertia contribution of the machine [10].
- Increased short-term overload capability: Depending on the type, a SC can provide more than twice its rating up to a few seconds, which enhances the system support during emergency situations or contingencies.
- Low-voltage ride through: Even under extreme low voltage contingencies, it remains connected and provides smooth, reliable operation.
- Fast response: By using modern excitation and control systems, a SC is fast enough to meet dynamic response requirements.
- Increased fault level: Another feature of a SC is that it provides real short-circuit power to the grid, improving the stability of the system with weak interconnections and the protection of the system.
- No harmonic content: A SC is not a source of harmonics and can even absorb harmonic currents. This feature enables ease of integration into existing networks.
- Decreased voltage unbalance levels: even if scarcely investigated in the technical literature [11], [12], the low negative sequence impedance of a SC provides a symmetry of phase voltages.

Typical applications of a SC include High Voltage Direct Current (HVDC) transmission systems which exploit the Line-Commutated Converter (LCC) technology [13]. In fact, SCs installed close to the converter station provide a fast dynamic reactive power support that helps to significantly reduce commutation failures of the converters [14], [15].

[1] Terna Rete Italia, 00156, Roma, Italy
[2] Department of Industrial Engineering, University of Padova, 35131 PD, Italy
[3] Correspondence email: domenico.tedeschi@terna.it
© 2025 Author(s). This is an open access article licensed under the Creative Commons Attribution License 4.0. (http://creativecommons.org/licenses/by/4.0/).

The installation of SC is also crucial for the feasibility of a power system restoration process which exploits HVDC-LCC corridors, to ensure the thyristor commutation in the receiving station during the black-start process. [16]–[19].

Disadvantages related to SC installations include higher level of loss, mechanical wear, and a slower response time compared to inverter-based technologies. It is important to note that over the last three decades, technologies based on highly dynamic, low-loss, and low-maintenance power electronic solutions, such as Static Var Compensator (SVC), have been preferred to Alternate Current (AC) technologies. Despite this, today, in a power system with a massive penetration of RES, the SCs installation again constitutes a robust solution to ensure system stability and thus plays a key role in the planning of future grid expansions [20], [21].

Motivation

Given the growing number of SC installations around the world, this work aims to investigate a critical aspect of the SC operation, i.e., the start-up process and its synchronization with the network.

Currently, the start-up process of a SC can be performed in two different ways. With medium-size SCs, the condenser is driven by a controlled motor to allow a precise electric parallel with a limited slip. Otherwise, for large-size SCs, a nondeterministic method is adopted. This second method, object of the present work, involves the use of a Static Frequency Converter (SFC) [22] to speed-up the SC from zero-frequency up to the nominal frequency, but for the grid synchronization the SFC must be disconnected and the electric parallel with the grid is carried out under freewheeling conditions. A controlled synchronization would require the use of a full-scale converter sized for the nominal voltage of the machine, which would be too expensive and consequently never available in practice.

For this reason, the actual strategy to perform the SC synchronization takes the machine to an over-frequency point and then disconnects the SFC, causing a freewheeling behavior until the reach of the optimal synchronization conditions. During this uncontrolled process the optimal conditions in terms of angle deviation, frequency deviation, and voltage deviation respect to the grid are not always reached, so resulting in a low Synchronization Success Rate (SSR) of the start-up attempts.

A common practice to increase the SSR of the process is to increase the allowed frequency threshold for synchronization, but in this way the mechanical and thermal stresses on the machine shaft are higher, with negative effects on the aging of the entire SC system. This work focuses on the synchronization method adopted for large-sized SCs.

Literature review

Until now in the scientific literature, only a few empirically based strategies have been proposed to increase the SSR.

In [23], an evaluation index for the synchronization of the SCs under different variable frequency start-up controls has been proposed. In particular, the paper proposes a hybrid start-up control scheme by merging slope-type-based control and a stair-type-based control with a step-type one. This method has been validated in a simulation environment.

Ref. [24] proposes three different criteria to control the start-up strategy and the synchronization process of a SC, based on the initial falling speed, the frequency difference, and the phase difference.

These studies only suggest predefined thresholds to perform the SFC disconnection to increase the SSR, based on parametric simulations, without deriving any deterministic result.

In [25], a new method to increase the SSR of the SC synchronization process is derived. The method proposes to regulate the freewheeling speed ratio of the SC by controlling its self-excitation current, or to modify the starting freewheel point frequency. The focus of the study is to dynamically modify the maximum speed of the machine by means of a trial-and-error procedure, without a deterministic derivation. This study shows promising results but does not benefit from experimental validation.
Recently, some of the authors in [26] approach the problem in a different way. They try to exploit the law of the uniform deceleration motion to analytically derive the conditions to perform a successful electric parallel. The method has been proven to correctly estimate a-priori the synchronization conditions by a preliminary comparison with real start-up processes.

Contribution

In the present paper, starting from the innovative approach proposed in [26], a complete deterministic procedure, called Deterministic Target Synchronization (DTS), is implemented.
The main contribution of this work with respect to the existing methodologies is threefold:

- The proposed procedure aims to analytically reproduce the freewheeling characteristic of the SC during the start-up process to derive the optimal frequency and phase conditions between the network and SC at which the SFC must be disconnected to guarantee a successful grid parallel in every operating condition.
- An additional adaptive control is derived, to dynamically update the exciter reconnection instant based on the value of the actual grid frequency value.

ISSN:2566-3143, eISSN:2566-3151, DOI: 10.2478/bhee-2026-0020

- The accuracy of the proposed method is confirmed by the comparison with many on-field recordings of real SC start-up processes.

Different methodologies proposed in literature are based on trial-and-error procedures or on parametric analyses, without any analytical derivation. In addition, these methods have never been validated in real-world scenarios.

The proposed approach allows avoiding synchronization failures and to push the SSR value close to 1 (SSR ∊ [0,1]). Moreover, it helps to strongly reduce mechanical and thermal stresses on the SC, by decreasing the frequency slip set in the synchro-check device, so to increase the lifetime of the machine.

It is as simple as effective, and it is very easy to integrate into the commercial devices which control the SC synchronization with the network. In fact, there is no need to modify the machine exciter control system [25], since the proposed method only determines the time instant when the SFC should be disconnected and the time instant when the exciter must be reconnected. This feature is very effective since it allows to easily integrate the present procedure in all the already connected SC plants.

Moreover, for the first time in scientific literature, the analytical model is validated by means of several on-field recordings of real synchronization tests performed on three different plants.

1. CLASSICAL SC SYNCHRONIZATION PROCESS

As mentioned above, to date, the synchronization procedure between a SC and the grid is based on a non-deterministic approach. Figure 1 shows the single line diagram of the portion of the SC plant involved in the machine start-up process. The process involves the SFC device, to increase the SC angular speed in the first part of the process; the exciter with a specific control; the Synchro-check device (ANSI 25), which monitors electrical quantities at the General Circuit Breaker (GCB) terminals and produces the control signal for the synchronization. The switch SW1 allows the connection between the SC stator winding and the SFC. The GCB is the switch between the SC and the step-up transformer.

Figure 2 reports an example of a real start-up sequence of a SC, derived by an on-field recording, in which the final part of the SC dynamic transition from zero-frequency until synchronization with the grid is represented. The orange band indicates the frequency range in which the synchronization is allowed, the red line represents the network frequency, and the blue line indicates the frequency corresponding to the SC speed.

The start-up procedure starts with the GCB and the SW1 open (see Fig. 1). The absence of a supply system capable of controlling the machine speed (differently from the case of a traditional synchronous generator) forces the use of a SFC [22] to control the process.

The SFC is initially connected to the SC stator (SW1 closed) so the machine works as a motor to increase the angular speed of the rotating parts (rotor shaft and, in some cases, flywheel system). Since the synchronization of the SC with the grid cannot be performed while the SFC is still connected (the network voltage applied to the SC bus would destroy the SFC), it is necessary to accelerate the machine over the grid frequency set-point.

During this phase, SFC controls the static exciter to set the voltage on the stator windings to approximately 15% of its nominal voltage.

Then, to allow the safety disconnection of the SFC and to preserve the exciter from damage, the following maneuvers are performed simultaneously:
- The exciter is turned off.
- The SFC outer thyristors are turned off.
- The SW1 is opened.

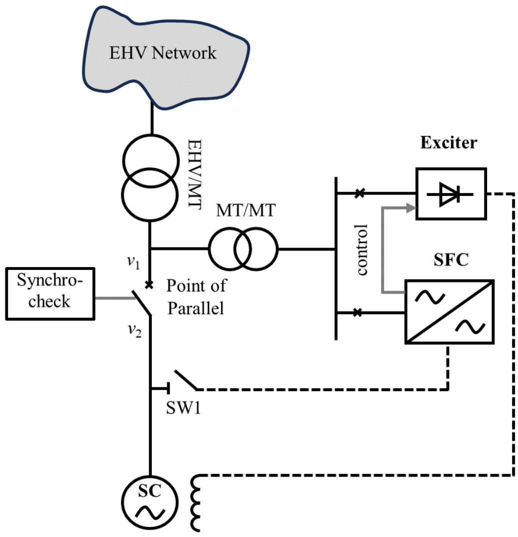

Figure 1: Single Line diagram of the portion of the SC plant involved in the start-up process of the machine.

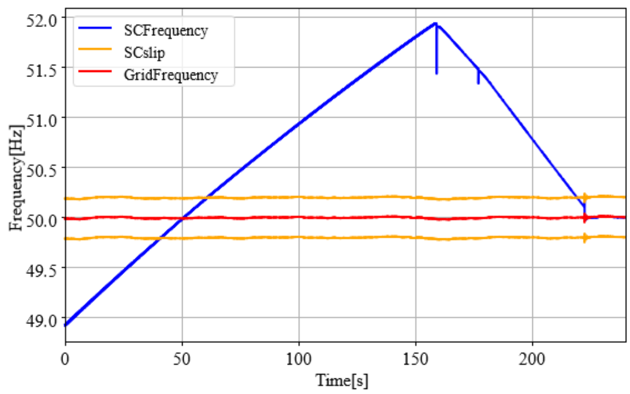

Figure 2: Recorded sequence of a start-up procedure.

Just after these operations, the machine speed starts to decrease freewheeling, and after few seconds (typically 18 s) the exciter is turned on and set to reach the nominal voltage on the stator windings. The speed decrease evolves until the machine simultaneously satisfies the conditions that allow the synchronization with the grid set on the Synchro-check device. The three conditions to be satisfied at the interface between the grid side voltage, called v1, and the SC side voltage, called v2, are typically set in the following ranges:

- The voltage magnitude difference within ±10%.
- The frequency slip s below 0.5%.
- The voltage angle difference within ±5 deg.

From Figure 3 it is also possible to observe the behavior of the voltage |v2| during the entire process (indicated in green in Fig. 3). Before the SFC disconnect its value is around 15% of its nominal value, then it exponentially decreases to zero to finally increase linearly to its nominal value when the exciter is turned on.

It should be noted that, before the electric parallel with the network, the value of v2 is proportional to the field current if supplied by the exciter, except when v2 exponentially decrease after the SFC disconnection. In fact, this phenomenon is due to the residual magnetization of the machine core, but it does not have a direct correlation with the field current, which goes instantaneously to zero when the exciter is turned off.

This actual start-up procedure of a SC presents two main problems: first, there is no indication on which could be the correct speed to push the generator before disconnecting the SFC, and secondly there is no assurance to obtain the relative phase condition needed to execute the main switch closing command when the SC frequency crosses

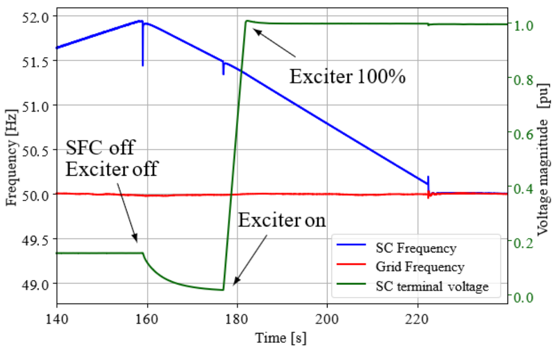

Figure 3: Final part of the SC start-up procedure where also the stator winding voltage of the SC is reported.

the grid frequency. In fact, it is not rare that a parallel procedure fails because the angle condition is not satisfied within the frequency slip. In this situation, the procedure must be repeated from scratch, with an unavoidably increase in the Operation & Maintenance (O&M) costs.

To obtain a higher SSR, the commonly accepted solution is to increase the frequency slip allowed for the synchronization device. However, a higher frequency slip introduces another problem related to the SC resilience, since every time a parallel is performed, the thermal and mechanical stresses are higher. This issue becomes worse when SC is designed without flywheel, because in this case the acceleration after disconnection of SFC is higher (since the inertia of the rotating masses is lower) and the frequency slip must be set to an even higher value to achieve synchronization. This allows the increasing of SSR but also increases the mechanical and thermal stress of the machine.

2. PROCESS CHARACTERIZATION

From the observation of real recordings of a SC synchronization process (see Fig. 3 as a reference) expounded in the previous section, it emerges that the fall speed of SC can be divided into three main stretches having different dynamics.

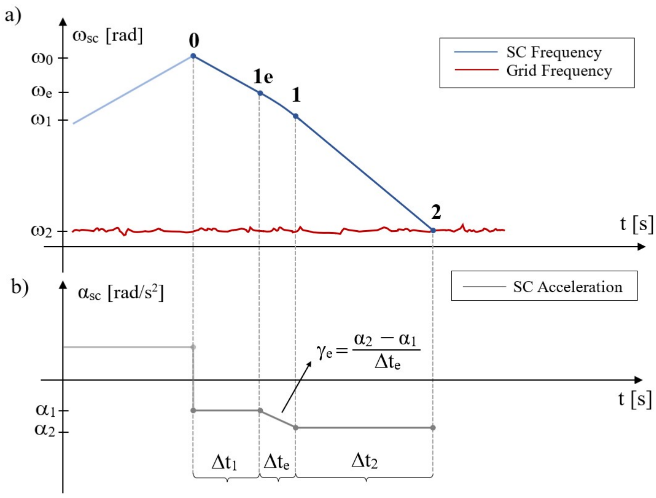

Figure 4: Analytical representation of the start-up process of a SC. a) angular speed profile b) acceleration profile.

Figure 4 schematically reproduces the SC angular speed (Figure 4a) and the SC acceleration (Figure 4b) for these three phases. The main stretches can be described as follows:

- **Section 0 - 1e**: In this phase, just after the disconnection of the SFC, the excitation is disconnected to allow the safety opening of the switch between the SFC the SC. Since the deceleration is constant, it is possible to assume a uniformly decelerated circular motion to find the solutions of SC angular speed and electric angle in the point 1e, starting from point 0, as follows:

$$\begin{cases} \vartheta_e = \vartheta_0 + (\omega_0 - \omega_{ref})\Delta t_1 + \frac{1}{2}\alpha_1 \Delta t_1^2 \\ \omega_e = \omega_0 + \alpha_1 \Delta t_1 \end{cases} \qquad (1)$$

where α_1 is the constant acceleration of the rotor shaft in the first phase, ϑ_0 and ϑ_e are the angle displacements between the SC phase voltage angle and the angle of the grid voltage ϑ_{ref} (which is the reference angle of the system, i.e., $\vartheta_{ref} = 0$)) in point 0 and point 1e, respectively; ω_{ref} is the reference speed and corresponds to the network frequency f_{ref} , i.e., $\omega_{ref} = 2\pi f_{ref}$; ω_0 and ω_e are the angular speeds of the SC in the two operating points and Δt_1 is time window of the section.

- **Section 1e – 1**: In this second phase, the exciter is restarted and so the field current goes from 0 to 1 pu. The acceleration decreases linearly in the time window. By assuming that α_2 is the acceleration when the field current reaches 1 pu, the angular speed ω_1 at point 1 can be derived as follows:

$$\omega_1 = \omega_e + \int_0^{\Delta t_e} \frac{\alpha_2 - \alpha_1}{\Delta t_e} t\,dt = \omega_e - \int_0^{\Delta t_e} \gamma_e t\,dt \qquad (2)$$

where Δt_e is the time frame of this section and γ_e is the differential of the acceleration $\alpha_{sc}(t)$ in that time frame. By solving (2), it is possible to derive an equivalent acceleration, called α_e, which is the mean value of α_1 and α_2 as follows:

$$\int_0^{\Delta t_e} \gamma_e t\,dt = \frac{1}{2}\gamma_e \Delta t_e^2 = \frac{1}{2}(\alpha_2 - \alpha_1)\Delta t_e = \alpha_e \Delta t_e \qquad (3)$$

Thus, the solutions in terms of angular speed and electric angle at point 1 can be derived, similarly to (1), as follows:

$$\begin{cases} \vartheta_1 = \vartheta_e + (\omega_e - \omega_{ref})\Delta t_e + \frac{1}{2}\alpha_e \Delta t_e^2 \\ \omega_1 = \omega_e + \alpha_e \Delta t_e \end{cases} \qquad (4)$$

where ϑ_1 is the voltage angle displacement and ω_1 is the angular speeds of the SC in point 1.

- **Section 1 – 2**: In this phase, the field current has reached its nominal value. As for the section 0-1e, it is possible to assume a uniformly decelerated circular motion:

$$\begin{cases} \vartheta_2 = \vartheta_1 + (\omega_1 - \omega_{ref})\Delta t_2 + \frac{1}{2}\alpha_2 \Delta t_2^2 \\ \omega_2 = \omega_1 + \alpha_2 \Delta t_2 \end{cases} \qquad (5)$$

where $\vartheta_2 = \vartheta_{ref}$, ω_2 is the angular speed corresponding to the network frequency f_{ref} , i.e., $\omega_2 = 2\pi f_{ref}$ and Δt_2 is time window of the section.

3. PROCESS PARAMETRIZATION

The purpose of this subsection is to describe the parametrization process of the analytical model consisting of (1), (4) and (5).

The approach to parameterize the model is a measurement-based approach, which exploits the recording performed on each specific SC object of the analysis.

In fact, during the commissioning of a SC, several tests are performed, and the test of the white parallel , i.e., the execution of the whole start-up procedure without issuing the closing command of the main switch (the equivalent of a failed parallel). Figure 5 shows an example of a white parallel test performed on a real SC.

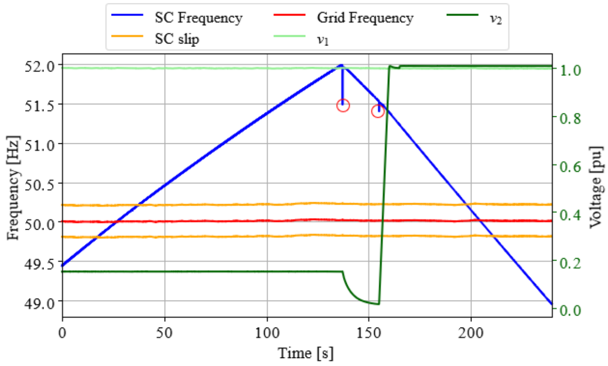

Figure 5: Example of a white parallel process

The two voltage signals provided by the measurement allow one to derive the instantaneous value of voltage, frequency, frequency derivative, and phase of the two sides (grid and SC).

The grid voltage signal v_1 acts as a reference, so its phase is 0, and the SC phase v_2 is measured compared with the v_1 phase. The recordings acquired on field always show points of discontinuity in the SC frequency corresponding to the opening or closing command of the medium voltage power breakers, which is a part of the process (see red circles in Figure 5). For this reason, in those points the registrations cannot be used to know the values of the real frequency and phase of the SC. However, the voltage module is read without undergoing distortions due to the MV commands already mentioned. Moreover, the recordings also make available the time derivative of the SC frequency, named dfsc.

The parametrization of the SC descending curve can now be derived. As reported in Figure 6, the main time instants extracted from the recordings are as follows:

- t_0: The initial instant of the descent sequence is identified when the SC voltage starts to drop from the constant of $|v_2| = 0.15$.
- t_e: A second point is identified when the exciter is restarted. This point also coincides with the minimum value of the SC voltage V_{2min}.
- t_1: The third point is detected after a few seconds when the nominal stator voltage value is reached ($|v_2| = 1$).
- t_2: The fourth and final point is captured at the equality of generator and grid frequencies.

The four identified time instants allow us to calculate the following parameters:

[1] The white parallel is performed as a standard parallel procedure, where the closing command is inhibited by opening command terminals. This allows checking the overall procedure in a safety mode without executing the real command.

$$
\begin{aligned}
\Delta t_1 &= t_e - t_0 \\
\Delta t_e &= t_1 - t_e \\
\alpha_1 &= 2\pi \cdot \overline{df_{sc}(t)} \quad \text{for} \quad t_0 < t < t_e \\
\alpha_2 &= 2\pi \cdot \overline{df_{sc}(t)} \quad \text{for} \quad t_1 < t < t_2 \\
\alpha_e &= \frac{\alpha_2 - \alpha_1}{2}
\end{aligned} \tag{6}
$$

where the overline symbol x indicates the mean value of the signal x for the specified interval. The last parameter Δt_2 is derived from the procedure explained in the following section.

The parametrization process is crucial for the correct characterization of the machine, to compute the optimal condition to start the synchronization process. Nevertheless, if some parameter is not available, it is possible to estimate them by the knowledge of the inertia of the rotating masses (for coefficients α_1), the data sheet of the excitation system (for coefficient α_2 and so α_e and Δt_e) and the actual timing of the excitation issuing command (for interval Δt_1).

4. DETERMINISTIC TARGET SYNCHRONIZATION (DTS)

The procedure to determine the optimal conditions to perform the parallel of SC with the network starts from the analytical model and the parametrization expounded in the previous section. It is worth noting that the procedure remains valid also for a SC coupled with flywheel. In this case, the coefficients α_1, α_e and α_2 will results lower in module for the increased inertia of the rotating masses.

4.1. Unconstrained Initial Conditions

The entire system to be solved can be derived based on (1), (4) and (5); furthermore, a seventh equation is added to link (4) and (5):

$$
\begin{cases}
\vartheta_e = \vartheta_0 + (\omega_0 - \omega_2)\Delta t_1 + \frac{1}{2}\alpha_1 \Delta t_1^2 \\
\omega_e = \omega_0 + \alpha_1 \Delta t_1 \\
\vartheta_1 = \vartheta_e + (\omega_e - \omega_2)\Delta t_e + \frac{1}{2}\alpha_e \Delta t_e^2 \\
\omega_1 = \omega_e + \alpha_e \Delta t_e \\
\vartheta_2 = \vartheta_1 + (\omega_1 - \omega_2)\Delta t_2 + \frac{1}{2}\alpha_2 \Delta t_2^2 \\
\omega_2 = \omega_1 + \alpha_2 \Delta t_2 \\
\vartheta_1 = -2k\pi
\end{cases} \tag{7}
$$

where ω_2 is the SC angular speed corresponding to the network frequency and k is a positive integer number. The last equation is added to constrain the voltage angle between SC and the network to perform at least k total revolution between points 1 and 2 during the time interval Δt_2.

The system (7) has seven equations and seven unknowns; thus, a unique solution can be derived if no further constraints are added. For this reason, this method has been called unconstrained initial conditions.

Starting from the last equation, by knowing the value of ω_2, α_2, α_e, α_1, Δt_e, and Δt_1 from the parametrization process, the system (7) can be solved to calculate the initial conditions to start the synchronization process, i.e., ϑ_0 and ω_0.

According to the previous section, the optimal target for the success of the synchronization is ensured by the condition ϑ_2= 0 when the SC frequency and the network frequency are equal. The first step is the computation of the time interval Δt_2 taking advantage of the last three equations of (7), where $\vartheta_2 = 0$:

$$
\begin{cases}
0 = -2k\pi + (\omega_1 - \omega_2)\Delta t_2 + \frac{1}{2}\alpha_2 \Delta t_2^2 \\
\omega_2 = \omega_1 + \alpha_2 \Delta t_2
\end{cases} \tag{8}
$$

The system solutions are the following:

$$
\begin{aligned}
\Delta t_2 &= \sqrt{-\frac{4k\pi}{\alpha_2}} \\
\omega_1 &= \omega_2 - \alpha_2 \Delta t_2
\end{aligned} \tag{9}
$$

To activate the synchro-check device, a minimum time Δt_{2min} must be considered before the SC reaches the point 2, so the following constraint must be satisfied:

$$\Delta t_2 > \Delta t_2^{min} \tag{10}$$

If the time interval Δt_2 is less than the time required to activate the synchro-check device, the value k of revolutions must be increased.

The final step is to determine the optimal condition at which the SC must be disconnected from the SFC. The pair of values ϑ_0 - ω_0 can be computed through the first four equations of (7):

$$
\begin{aligned}
\omega_e &= \omega_1 - \alpha_e \Delta t_e \\
\vartheta_e &= -2k\pi - (\omega_e - \omega_2)\Delta t_e - \frac{1}{2}\alpha_e \Delta t_e^2 \\
\omega_0 &= \omega_e - \alpha_1 \Delta t_1 \\
\vartheta_0 &= \vartheta_e - (\omega_0 - \omega_2)\Delta t_1 - \frac{1}{2}\alpha_1 \Delta t_1^2
\end{aligned} \tag{11}
$$

For a set of known and fixed quantities (i.e., α_1, α_2, α_e, Δt_e, Δt_1, ω_2), different pair of values of ϑ_0 - ω_0 can be obtained by varying the number of total revolutions k during the time interval Δt_2. The number of total revolutions has an impact on the angular speed ω_1 and through (11) on ϑ_0 and ω_0. Multiple values of ω_0 can be computed by considering the extension of by summing $2k\pi$ with an integer value of k. It is interesting to derive the optimal speed ω_0 of the starting sequence by DTS for different values of k, to study how the speed characteristic changes when the time interval Δt_2 increases.

ISSN:2566-3143, eISSN:2566-3151, DOI: 10.2478/bhee-2026-0020

As represented in Figure 6, the increase in k affects the initial speed ω_0 less and less, as the time increase is proportional to the square root of k. In Table I, the main synchronization parameters obtained by varying k are reported. It is possible to observe that the initial angle interval, named $\Delta\vartheta_0$, for which the parallel is successful does not depend on the initial speed of the SC, ω_0.

Starting from the just-presented method, another one can be developed by imposing the angular speed ω_0 at which the SC must be disconnected from the SFC. Furthermore, an adaptive method to adjust the interval Δt_1 is reported. The present method modifies the instant when the exciter is reconnected to the SC to consider any disturbances in the network frequency during the interval between the points 0 and 1e. This technique helps to increase the SSR value.

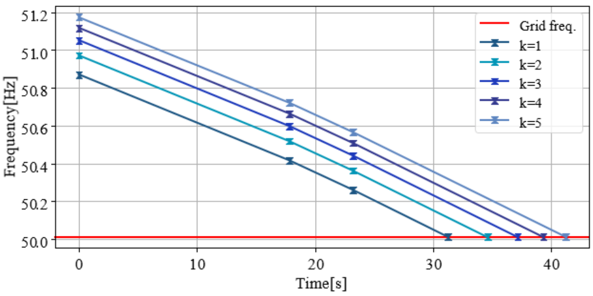

Figure 6: Parametric analysis to derive the speed characteristic by DTS varying the value of k for Test #1.

Table I. Main synchronization parameters for different values of k.

k	Δt_2 [s]	ω_0 [Hz]	ϑ_0 [deg]	$\Delta\vartheta_0$ [deg]
1	8.04	50.87	355	234
2	11.40	50.97	216	234
3	13.95	51.05	276	234
4	16.11	51.12	80	234
5	18.01	51.18	310	234

4.2. Constrained ω_0 method

This approach calculates the optimal SC angle ϑ_0 to start the synchronization when the initial angular speed ω_0 is imposed. The set of equations (7) must be modified since the SC voltage angle does not complete an integer number k of revolutions with respect to the network during the Δt_2 time interval. Hence, the last formulation of (7) is removed. The duration of the Δt_2 time interval can be adjusted by varying the initial angular speed ω_0. As in the previous method, the optimal target for the success of the synchronization is ensured by the condition $\vartheta_2 = 0$ when the SC frequency and the network frequency are equal. The equations reported in (7) are still valid and must be solved to determine ϑ_0, ϑ_e, ω_e, ϑ_1, ω_1 and Δt_2. By exploiting the second, the fourth and the sixth equation of (7), Δt_2 can be assessed:

$$\Delta t_2 = \frac{\omega_2 - \omega_0}{\alpha_2} - \frac{\alpha_1}{\alpha_2}\Delta t_1 - \frac{\alpha_e}{\alpha_2}\Delta t_e \tag{12}$$

If the constraint (10) is not satisfied, the initial angular speed ω_0 must be increased. Once the time interval Δt_2 is computed, all the unknown rotor angles can be computed:

$$\begin{aligned}
\vartheta_1 &= -(\omega_e - \omega_2)\Delta t_2 - \frac{1}{2}\alpha_2 \Delta t_2^2 \\
\vartheta_e &= \vartheta_1 - (\omega_e - \omega_2)\Delta t_e - \frac{1}{2}\alpha_e \Delta t_e^2 \\
\vartheta_0 &= \vartheta_e - (\omega_0 - \omega_2)\Delta t_1 - \frac{1}{2}\alpha_1 \Delta t_1^2
\end{aligned} \tag{13}$$

As in the previous method, it is possible to derive a set of ϑ_0 angles by modifying a constrained input parameter. It could be appropriate to select the minimum angular speed ω_0 that satisfies (10) to minimize the mechanical stress due to overspeed.

4.3. Adaptive method

In real operation scenarios, during the synchronization procedure, the network frequency could vary due to a power imbalance between generation plants and end-users. As already seen in the previous methods, the initial conditions to start the procedures can be computed starting from the network frequency ω_2 by means of (9)-(11) or (12)-(13).

The network frequency adopted in these equations is the real one derived from the grid-side voltage measurement, and it is continuously updated. Once the synchronization procedure starts at point 0, the network frequency variation could have an impact on the SSR. To increase SSR value, the duration of the first-time interval (i.e., between the point 0 and the point 1e) can be adapted to consider the disturbances in the network frequency. For instance, if the network frequency increases compared to that at point 0, the Δt_1 value is reduced.

The procedure developed in the following allows computing the instant te when the exciter is reconnected to the SC (i.e., the interval Δt_1), to update the duration of this interval based on fluctuations in the network frequency.

Since during this time interval some operations must be performed, a minimum time interval Δt_1^{min} is required.

Therefore, the interval Δt_1 of (11), (12) and (13) must be increased so that the new $\Delta t_1(\omega_2)$ calculated by the adaptive method is greater than the minimum time interval. When the adaptive method is activated, the increased time interval adopted in (11), (12) and (13) is identified by the symbol Δt_1^0.

The increased time interval can be computed with the following expression:

$$\Delta t_1^0 = \Delta t_1^{min} + \frac{\omega_2 - \omega_2^{max}}{\alpha_1} \tag{14}$$

where Δt_1 is the minimum time interval and ω_2^{max} is the angular speed corresponding to the maximum frequency that the network can reach during standard operation.

Once the synchronization process starts, the time interval Δt_1(t), which depends on the angular speed related to the real time frequency ω_2(t), can be calculated by solving the following set of equations:

$$\begin{cases} \omega_2(t) = \omega_1(t) + \alpha_2 \Delta t_2 \\ \omega_1(t) = \omega_e(t) + \alpha_e \Delta t_e \\ \omega_e(t) = \omega_0 + \alpha_1 \Delta t_1(t) \end{cases} \tag{15}$$

In (15), ω_0 is the SC angular speed when the synchronization procedure starts, Δt_e and Δt_2 are the time intervals adopted in (9)-(11) or in (12)-(13) (depending on the method considered).

Thus, the time interval $\Delta t_2(\omega_2)$ is equal to:

$$\Delta t_1(t) = \frac{\omega_2(t) - \omega_0}{\alpha_1} - \frac{\alpha_2}{\alpha_1}\Delta t_2 - \frac{\alpha_e}{\alpha_1}\Delta t_e \tag{16}$$

Eq. (16) can be cyclically computed by updating the real-time measurement of ω_2(t) until the following condition is valid:

$$\Delta t_1(t) < t \tag{17}$$

where time counting starts at the beginning of the synchronization procedure, i.e. $t_0 = 0$. When (16) returns a value equal to t, the exciter can be reconnected to the SC. All these procedures have been implemented in a Python-based program named DTS. The software includes a Graphical User Interface (GUI) useful to upload the measurement files needed to parameterize the SC behavior and to extrapolate the values of α_1, α_2, and Δt_1. Then, it can perform the analysis of the transient dynamics of the SC and to determine which should be the maximum optimal angle and speed for each of the operation methods expounded in this section to ensure a safe and successful network synchronization.

For the practical implementation, the idea is to use DTS parametrization step for the characterization of the SC machine to identify the parameters necessary for the application of the method in a real case. This step is made only one time and it is performed during the commissioning tests, for new SC, or during a SC downtime, for an already connected SC.

Subsequently, the core of the algorithm, which determines the optimal angle and speed to start the descending phase, is implemented in a system that controls both SFC and the excitation system. The method is applicable both SC with and without freewheel.

5. ANALYSIS OF REAL SYNCHRONIZATION PROCESSES BY (DTS)

This section presents the analyses of real on-field SC start-up processes to verify the effectiveness of the proposed analytical model. The aim is to compare the measurements of several SC synchronizations of different machines with the SC phase and the speed estimated by DTS. Moreover, different parametric analyses demonstrate how the on-field implementation of DTS can significantly increase the SSR of the SC grid synchronization.

The recordings are performed during synchronization tests on three SCs owned by the Italian TSO Terna, named SC1, SC2 and SC3. These machines are all equipped with flywheel under vacuum to increase their inertia and are currently in operation and connected to the Italian Transmission Network (TN). These machines have been designed to comply with a Terna standardized project, with a rated power of +250/125 MVAR, a nominal voltage of 19 kV, a starting time of the rotating masses of 14 s and the step-up transformer has a rated power of 290 MVA. The instrument adopted for the recordings is an Omicron CMC430 device with a sample rate of 10 kHz.

In Figure 7, a top view of the plant where SC2 and SC3 are installed is shown.

The available recordings are related to ten synchronization tests (six tests on SC1, two tests on SC2, and two tests on SC3), four of which are unsuccessful, and the others are successful. It should be noted that these tests have been performed before the implementation of DTS, nevertheless, they are very useful to verify the response of the analytical model proposed in the paper. The setup conditions for the 10 tests are reported in Table II. The synchronization process of the three machines has been parametrized according to the procedure described in the previous section, and the derived parameters are reported in Table III.

Figure 7: Top view of the SC2 and SC3 plant.

Figures 8 and 9 show the comparison between the recordings and the analytical results in terms of the angular speed and phase angle of the SC during the first failed test performed on SC1. The angular speed

ISSN:2566-3143, eISSN:2566-3151, DOI: 10.2478/bhee-2026-0020

of the SC in Figure 8 is converted to frequency by the well-known relation $f = \omega/2\pi$. The results show how the analytical model can reproduce the real behavior of a SC with a high accuracy. The error in estimating the initial phase ϑ_0 is in the order of 1 degree.

Table II. Set-up conditions of the 10 analyzed synchronization tests.

n. Test	n. SC	Success?	Slip s [%]	$\omega_{0,real}$ [Hz]	$\vartheta_{0,real}$ [deg]	$\Delta t_{2,real}$ [s]
#1	SC1	No	0.4	52.00	46	13.94
#2	SC1	Yes	0.4	51.94	138	13.92
#3	SC1	Yes	0.4	51.92	252	13.95
#4	SC1	Yes	0.4	51.97	194	13.94
#5	SC1	No	0.4	51.95	347	13.93
#6	SC1	No	0.4	51.97	286	13.95
#7	SC2	No	0.25	52.51	317	15.80
#8	SC2	Yes	0.45	52.51	175	15.80
#9	SC3	Yes	0.3	52.54	238	15.81
#10	SC3	Yes	0.45	52.54	69	15.83

Table III. Parametrization of the parallel phases after the disconnection of the SFC for the three SCs.

n. of machine	Δt_1 [s]	Δt_e [s]	α_1 [rad/s]	α_e [rad/s]	α_2 [rad/s]
SC1	17.85	5.38	-0.160	-0.175	-0,194
SC2	15.33	5.44	-0.124	-0.139	-0.152
SC3	17.56	5.41	-0.123	-0.137	-0.160

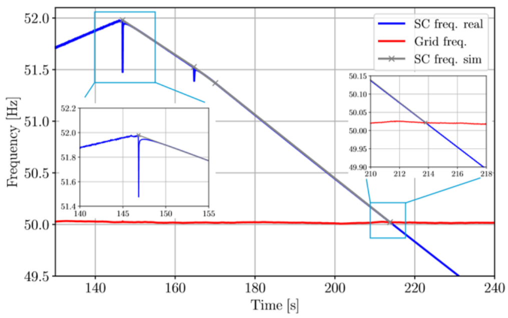

Figure 8: Comparison between recordings and analytical model in terms of frequency of the SC during a failed parallel test performed on SC1

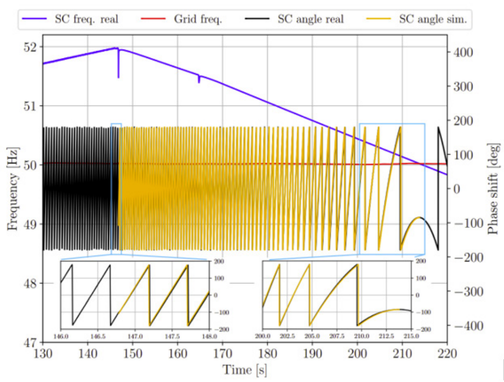

Figure 9: Comparison between recordings and analytical model in terms of phase shift of the SC during a failed parallel test performed on SC1.

Figure 10 reports the real phase angle ϑ_0 between the SC and the network in point 0 for the 10 synchronization tests.

The blue line represents the real angle ϑ_0 at which the SFC has been disconnected at speed ω_0 and the green band is the locus of angles at which the SFC would have been disconnected (at the same speed ω_0) to obtain a successful parallel within the allowable slip s, computed by DTS. It is interesting to observe that the green band also corresponds to the value of the SSR, i.e., the probability of performing a successful parallel.

In Figure 10, for all failed tests, the angle ϑ_0 is outside the green band; conversely, when the synchronization is successful, the angle is inside the green band. This perfect match confirms the accuracy of the model for the determination of the allowable conditions for a successful parallel.

It should be noted that the amplitude of the green area of the polar plots in Figure 10 is related to the slip frequency set in the synchro-check device. In fact, for lower slip the allowable phase interval to dump the SC in the starting point is smaller (see, e.g., tests #1- #7 or test #9), and for higher slip the allowable interval is larger (see, e.g., tests #8 and #10, for whom all starting phases are allowed).

High slips ensure an SSR≈1 but are critical since a parallel with high frequency difference could stress the SC and potentially damage the machine due to high mechanical and thermal stresses.

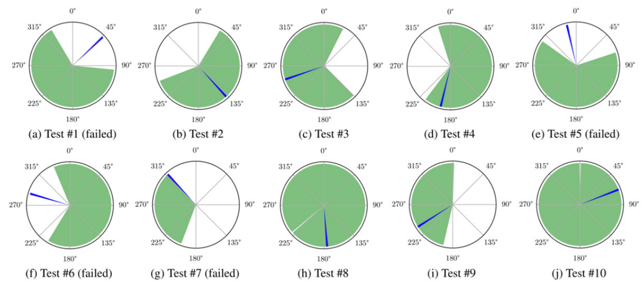

Figure 10: Polar representation of initial SC phase (blue) and of interval indicating the locus of the initial SC phases to obtain a successful parallel (green band). Each polar graph refers to a specific test reported in Table II.

Eventually, Figure 11 and Figure 12 show the predictive control applied to test #2 and to test #10, respectively. It can be observed how, starting from the same initial conditions (ϑ_0 - ω_0), the introduction of the predictive control method (black line) would have led to the network parallel with a lower slip compared to the parallel occurred (blue line), for both cases.

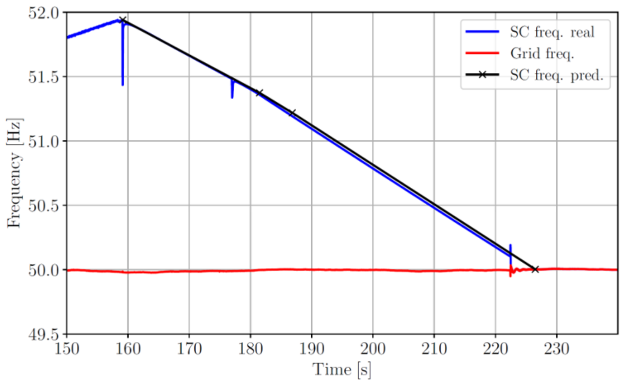

Figure 11: Predictive control applied to SC1 in the test #2.

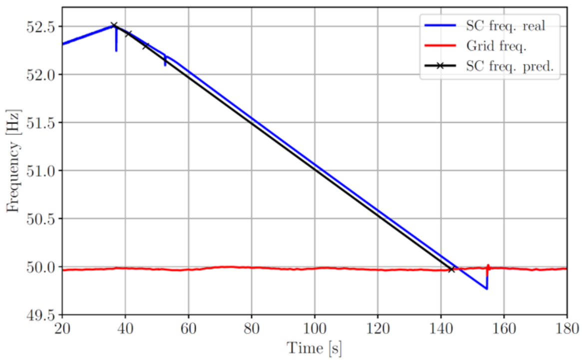

Figure 12: Predictive control applied to SC3 in the test #10.

6. CONCLUSION

In this work, for the first time in technical literature, the problem of the deterministic synchronization of SCs is addressed in a comprehensive manner. This research is a response to the increasing installations of SCs all over the world, which need a fast procedure for their integration in electrical grids to avoid failed synchronizations.

More specifically, the method is rooted in the equations of the uniformly accelerated circular motion supported by suitable simplifying hypotheses, and it can analytically determine the optimal frequency and phase angle conditions to ensure safe SC synchronization. Moreover, it can dynamically adapt the issuing of the exciter before the synchronization based on real-time grid frequency fluctuations.

All the above-mentioned procedures are embraced into a comprehensive Python-based tool called DTS. The analytical model is capable of reproducing recordings of real start-up processes with very good accuracy, and it could identify the reason behind the failure of several analyzed synchronization processes. Moreover, it can suggest the constraint to always obtain a successful parallel for a given SC.

By means of DTS, it is possible to significantly reduce the frequency slip set in the parallel device so to limit the thermal and mechanical stresses of the SC, ensuring a longer lifecycle with minimal impact on the actual setting of the parallel devices. The next step of the research is the implementation of DTS on the devices used to perform SC synchronization, which serves as a further validation of the proposed approach.

REFERENCES

[1] A. Carbonara, S. Dambone Sessa, A. L'Abbate, F. Sanniti, and R. Chiumeo, "Comparison of advanced flexible alternating current transmission system (FACTS) devices with conventional technologies for power system stability enhancement: An updated review," Electronics, vol. 13, no. 21, p. 4262, Oct. 2024.
[2] H. T. Nguyen, G. Yang, A. H. Nielsen, and P. H. Jensen, "Combination of synchronous condenser and synthetic inertia for frequency stability enhancement in low-inertia systems," IEEE Trans. Sustain. Energy, vol. 10, no. 3, pp. 997–1005, Jul. 2019.
[3] A. Stiger, R. A. Rivas, and M. Halonen, "Synchronous condensers contribution to inertia and short circuit current in cooperation with STATCOM," in Proc. IEEE PES GTD Grand Int. Conf. Expo. Asia (GTD Asia), Mar. 2019, pp. 955–959.
[4] C. Szabo, "An old tool rediscovered to address new grid challenges," Power Enginnering Int., Dec. 2017. [Online]. Available: https://www.powerengineeringint.com/news/an-old-tool-rediscovered-to- address-new-grid-challenges/
[5] SP Energy Netw. (Oct. 2019). Phoenix Internatinal Review. [Online]. Available: https://www.spenergynetworks.co.uk
[6] TenneT Commissions Three Grid Stabilization Systems for the German Power Grid, T&D World, Overland Park, KS, USA, 2022.
[7] Litgrid. (Jun. 2021). Development Plan of the Electric Power System and Transmission Grid 2021-2030. [Online]. Available: https://www.litgrid.eu/uploads/files /dir580/dir29/dir1/10_0.php
[8] Terna. (2023). Grid Development Plan 2023—Hypergrid Project. [Online]. Available: https://www.terna.it/en/electric-system/grid/national- electricity-transmission-grid-development-plan
[9] Elering. (Jun. 2023). Synchronization With Continental Europe. [Online]. Available: https://elering.ee/en/synchronization-continental-europe
[10] F. Palone, F. M. Gatta, A. Geri, S. Lauria, and M. Maccioni, "New synchronous condenser–flywheel systems for a decarbonized sardinian power system," in Proc. IEEE Milan PowerTech, Jun. 2019, pp. 1–6.
[11] L. Rusalen, G. Gardan, and R. Benato, "Application to the Italian AC/DC EHV network of the paduan three-phase power flow (PFPD_3P)," IEEE Trans. Ind. Appl., vol. 60, no. 6, pp. 8067–8076, Nov. 2024.

[12] R. Benato, G. Gardan, and L. Rusalen, "A three-phase power flow algorithm for transmission networks: A hybrid phase/sequence approach," IEEE Access, vol. 9, pp. 162633–162650, 2021.
[13] R. Benato and G. Gardan, "A novel AC/DC power flow: HVDC-LCC/VSC inclusion into the PFPD bus admittance matrix," IEEE Access, vol. 10, pp. 38123–38136, 2022.
[14] Y. Lei, T. Li, Q. Tang, Y. Wang, C. Yuan, X. Yang, and Y. Liu, "Comparison of UPFC, SVC and STATCOM in improving commutation failure immunity of LCC-HVDC systems," IEEE Access, vol. 8, pp. 135298–135307, 2020.
[15] J. Burr, S. Finney, and C. Booth, "Comparison of different technologies for improving commutation failure immunity index for LCC HVDC in weak AC systems," in Proc. 11th IET Int. Conf. AC DC Power Transmiss., 2015, pp. 1–7.
[16] L. Michi, E. M. Carlini, T. B. Scirocco, G. Bruno, R. Gnudi, C. Pisani, M. Salvetti, and D. Macalli, "The restoration field tests in sardinian network involving HVDC, synchronous condensers and hydraulic power plant," in Proc. AEIT HVDC Int. Conf. (AEIT HVDC), May 2019, pp. 1–5.
[17] R. Benato, S. Dambone Sessa, and F. Sanniti, "Lessons learnt from modelling and simulating the bottom-up power system restoration processes," Energies, vol. 15, no. 11, p. 4145, Jun. 2022.
[18] F. Sanniti, R. Benato, and F. Milano, "Participation of DERs to the bottom-up power system frequency restoration processes," IEEE Trans. Power Syst., vol. 38, no. 3, pp. 2630–2640, May 2023.
[19] Analysis of Low Frequency Oscillations Observed During a Power System Restoration Test," 2021 AEIT International Annual Conference (AEIT), Milan, Italy, 2021, pp. 1-6, doi: 10.23919/AEIT53387.2021.9626997.
[20] H2020 MIGRATE. (2020). The Massive Integration of Power Electronic Devices. [Online]. Available: https://www.h2020- migrate.eu/downloads.html
[21] F. O. Igbinovia, G. Fandi, Z. Muller, and J. Tlusty, "Reputation of the synchronous condenser technology in modern power grid," in Proc. Int. Conf. Power Syst. Technol. (POWERCON), Nov. 2018, pp. 2108–2115.
[22] T.-H. Liu, C.-Y. Lin, J.-S. Yang, and W.-Y. Chang, "Modeling and performance of a static frequency converter starting a 300 MVA synchronous machine," Electric Power Syst. Res., vol. 37, no. 1, pp. 45–53, Apr. 1996.
[23] P. Wang, Q. Mou, X. Liu, W. Gu, and X. Chen, "Start-up control of a synchronous condenser integrated HVDC system with power electronics based static frequency converter," IEEE Access, vol. 7, pp. 146914–146921, 2019.
[24] P. Wang, X. Liu, Q. Mou, W. Gu, and X. Zhao, "Start-up control and grid integration characteristics of 300 Mvar synchronous condenser with voltage sourced converter-based SFC," IEEE Access, vol. 7, pp. 176921–176934, 2019.
[25] Y. Sun, Z. Cao, Q. Wang, and S. Wang, "Improving grid-connection reliability and safety of synchronous condensers with start-up process optimization," IEEE Access, vol. 8, pp. 153742–153755, 2020.
[26] F. Sanniti, D. Tedeschi, L. Rusalen and R. Benato, "DTS: A New Deterministic Approach to Derive the Optimal Synchronization Conditions of a Synchronous Condenser," in IEEE Access, vol. 13, pp. 31936-31948, 2025, doi: 10.1109/ACCESS.2025.3542264.